

Supplementary Material
**Data-Driven Analyses of Rotational Energy-landscapes of Organic
Cation in Substituted Alloy Perovskite**

Wiwittawin Sukmas,^{1,2} Annop Ektarawong,^{3,2,*} Prutthipong Tsuppayakorn-ae,^{1,2}
Björn Alling,⁴ Udomsilp Pinsook,^{1,2} and Thiti Bovornratanaraks^{1,2,†}

¹*Extreme Conditions Physics Research Laboratory (ECPRL) and Physics of Energy Materials Research Unit (PEMRU),
Department of Physics, Faculty of Science, Chulalongkorn University, 10330 Bangkok, Thailand*

²*Thailand Center of Excellence in Physics, Ministry of Higher Education, Science,
Research and Innovation, 328 Si Ayutthaya Road, Bangkok 10400, Thailand*

³*Chula Intelligent and Complex Systems (CHICS), Department of Physics,
Faculty of Science, Chulalongkorn University, 10330 Bangkok, Thailand*

⁴*Theoretical Physics Division, Department of Physics, Chemistry,
and Biology (IFM), Linköping University, SE-581 83 Linköping, Sweden*

(Dated: November 19, 2020)

TABLE S1: Atomic fractional coordinates of MABiSeI

atoms	a	b	c
C1	0.596942024	0.491789991	0.499962968
N1	0.36140299	0.491952977	0.499827046
H1	0.655719988	0.656453955	0.499712993
H2	0.652230956	0.40883999	0.643757024
H3	0.652379008	0.408363996	0.356515996
H4	0.299061001	0.566852999	0.634274021
H5	0.299210986	0.566468997	0.365063006
H5	0.296755018	0.338210006	0.500002994
Bi	0.00000000	0.00000000	0.00000000
I1	0.50000000	0.00000000	0.00000000
I2	0.00000000	0.50000000	0.00000000
SeI	0.00000000	0.00000000	0.50000000

ATOMIC COORDINATES OF THE INPUT STRUCTURE OF CUBIC MABISEI

The cubic structure of $CH_3NH_3BiSeI_2$ or MABiSeI [1] with a lattice parameter of 6.28 Å consists of atoms as described in a table S1.

EULER'S ROTATIONS

The Euler's rotations are rigorously expressed by equation 1, where R and R' indicate the $(0^\circ, 0^\circ, 0^\circ)$ spatially-directed and the rotated atomic positions of the MA cation, respectively

$$\mathbf{R} = \lambda_\psi \lambda_\theta \lambda_\phi \mathbf{R}'$$

$$\begin{bmatrix} x \\ y \\ z \end{bmatrix} = \begin{bmatrix} \cos\psi & \sin\psi & 0 \\ -\sin\psi & \cos\psi & 0 \\ 0 & 0 & 1 \end{bmatrix} \begin{bmatrix} 1 & 0 & 0 \\ 0 & \cos\theta & \sin\theta \\ 0 & -\sin\theta & \cos\theta \end{bmatrix} \begin{bmatrix} \cos\phi & \sin\phi & 0 \\ -\sin\phi & \cos\phi & 0 \\ 0 & 0 & 1 \end{bmatrix} \begin{bmatrix} x' \\ y' \\ z' \end{bmatrix} \quad (1)$$

ENERGY LANDSCAPES

The orthogonality of the four-dimensional axes is preserved by introducing a set of cross-section that visualises three-dimensional energy topography. Variation of the total energies with respect to single Eulerian angles is reported in figure S1.

ψ – fixed schemes

Some selected landscapes in $E(\phi, \theta, \psi) = E(\phi, \theta, \psi + 180^\circ)$ relationship. Angles ψ are kept fixed when the total energies are plotted along the other angles, i.e., ϕ and θ , as shown in figures S2, S3, and S4.

θ – fixed schemes

Some selected landscapes in $E(\phi, 360^\circ - \theta, \psi) = E(\phi, \theta, \psi)$ relationship. Angles θ are kept fixed when the total energies are plotted along the other angles, i.e., ϕ and ψ , as shown in figures S5, S6, and S7.

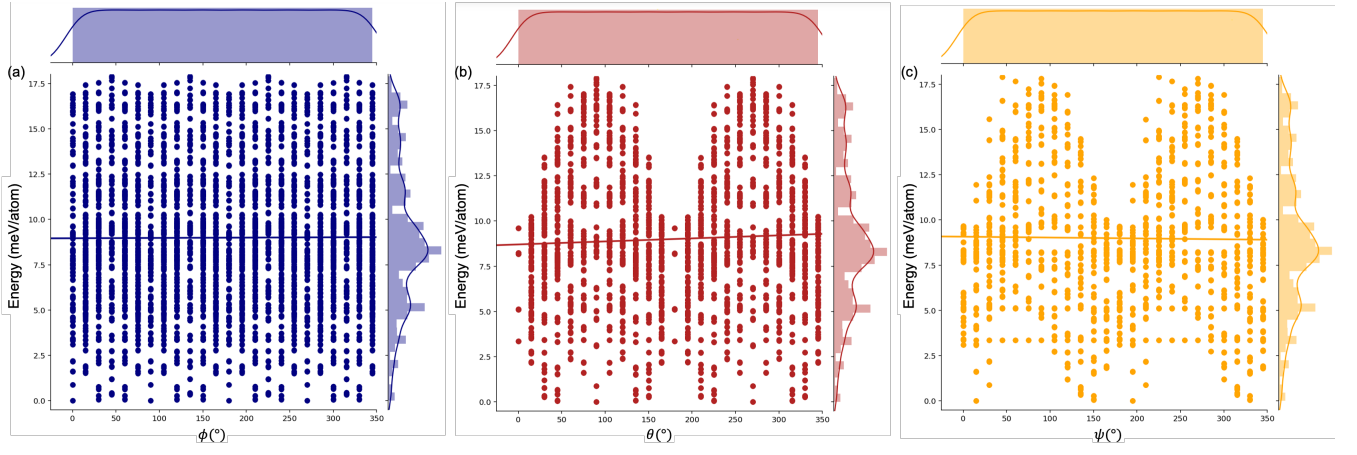
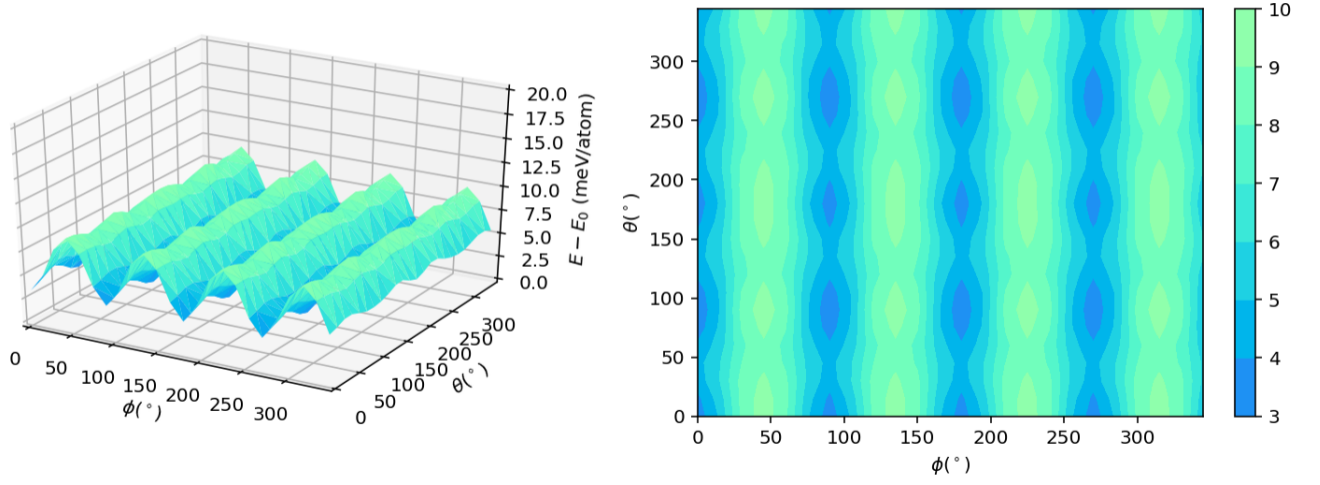
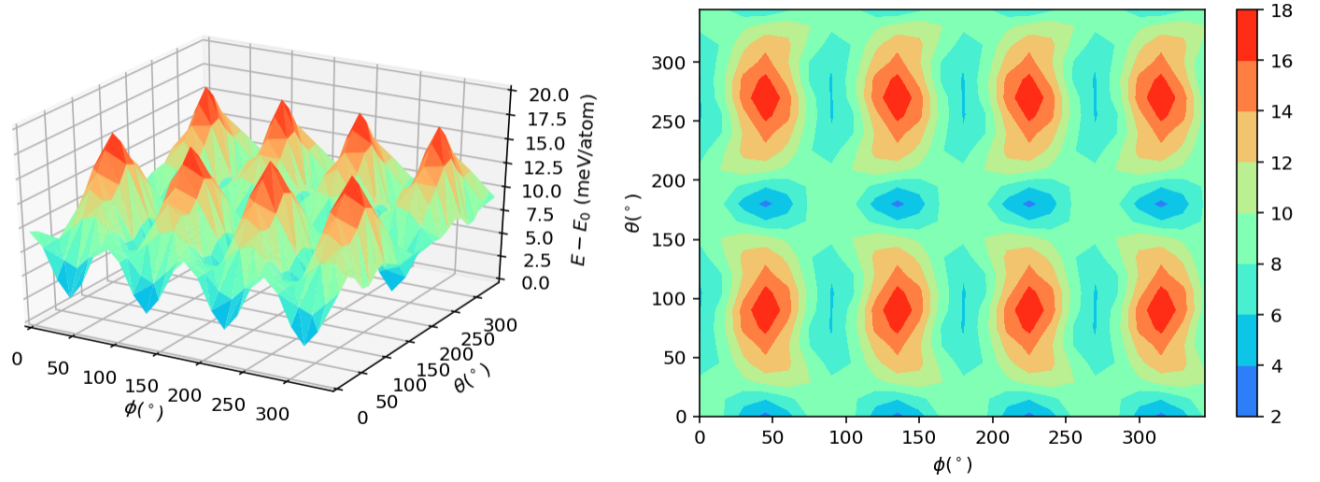


FIG. S1: Energy plotted along each angle

 $\psi = 0^\circ$
FIG. S2: Energy landscape corresponding to $E(\phi, \theta, \psi = 0^\circ)$
 $\psi = 45^\circ$
FIG. S3: Energy landscape corresponding to $E(\phi, \theta, \psi = 45^\circ)$

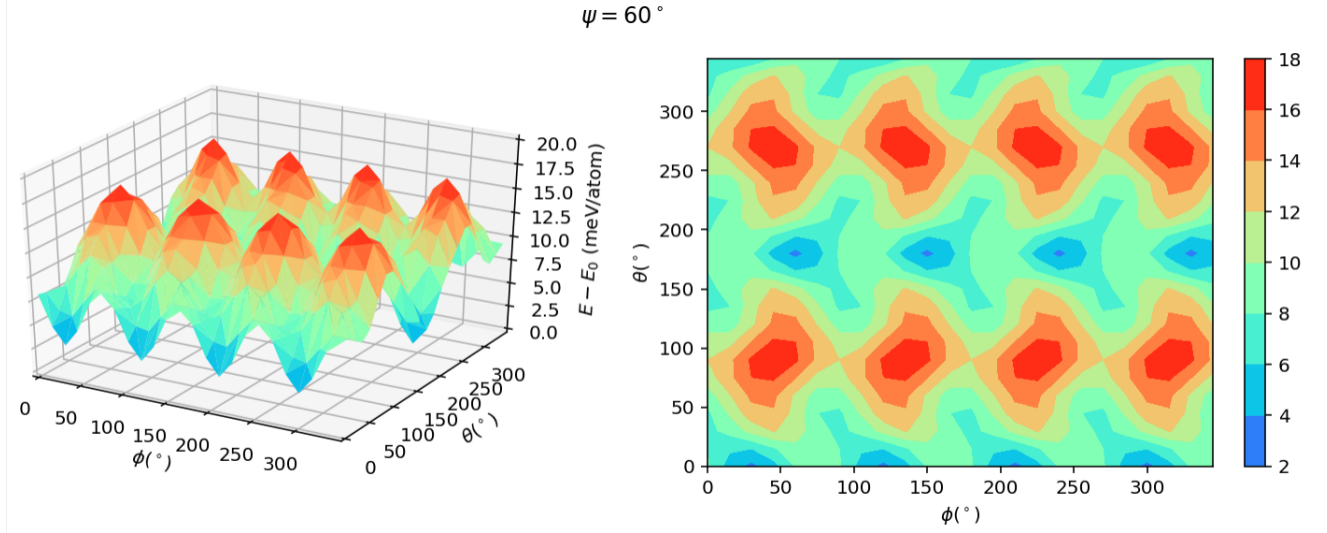


FIG. S4: Energy landscape corresponding to $E(\phi, \theta, \psi = 60^\circ)$

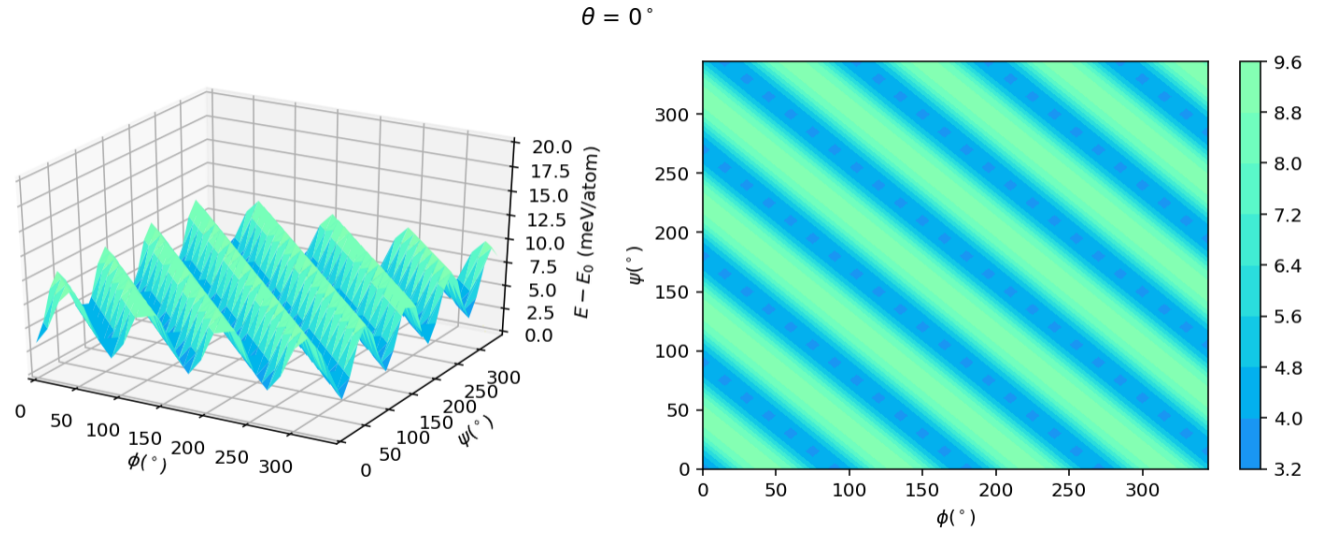


FIG. S5: Energy landscape corresponding to $E(\phi, \theta = 0^\circ, \psi)$

ϕ — fixed schemes

Some selected landscapes in $E(\phi + 180^\circ, \theta, \psi) = E(\phi, \theta, \psi)$ relationship. Angles ϕ are kept fixed when the total energies are plotted along the other angles, i.e., θ and ψ , as shown in figures S10, S11, and S12.

BONDLENGTHS AND ENERGY RELATIONSHIP

As earlier discussed, with increase in data dimensions the normal three-dimension geometric intuition fails quickly. All pairwise permutations corresponding to some selected pairs are reported in figure S13 along with their Pearson's correlations. Also, some selected pairs are delineated by means of the parallel coordinates in place of presenting all pairwise permutations. Therefore, instead of adopting a scheme attempting to preserve the orthogonality requirement of n -dimensional coordinate axes, parallel representation [2] is proposed to reveal some hidden messages in our data, as shown in figure S14. The values of each axis with its corresponding ΔE are distinguished by a colour gradient, while the range of which is intentionally selected to be 16 – 18 meV, avoiding too much relative homogeneity in energy

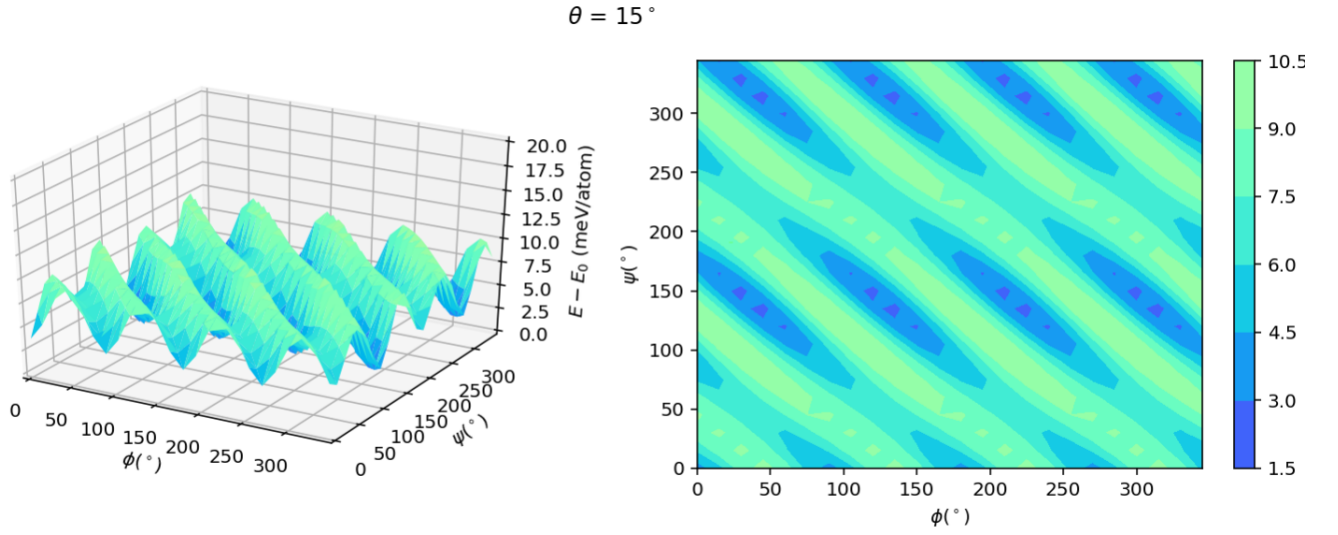


FIG. S6: Energy landscape corresponding to $E(\phi, \theta = 15^\circ, \psi)$

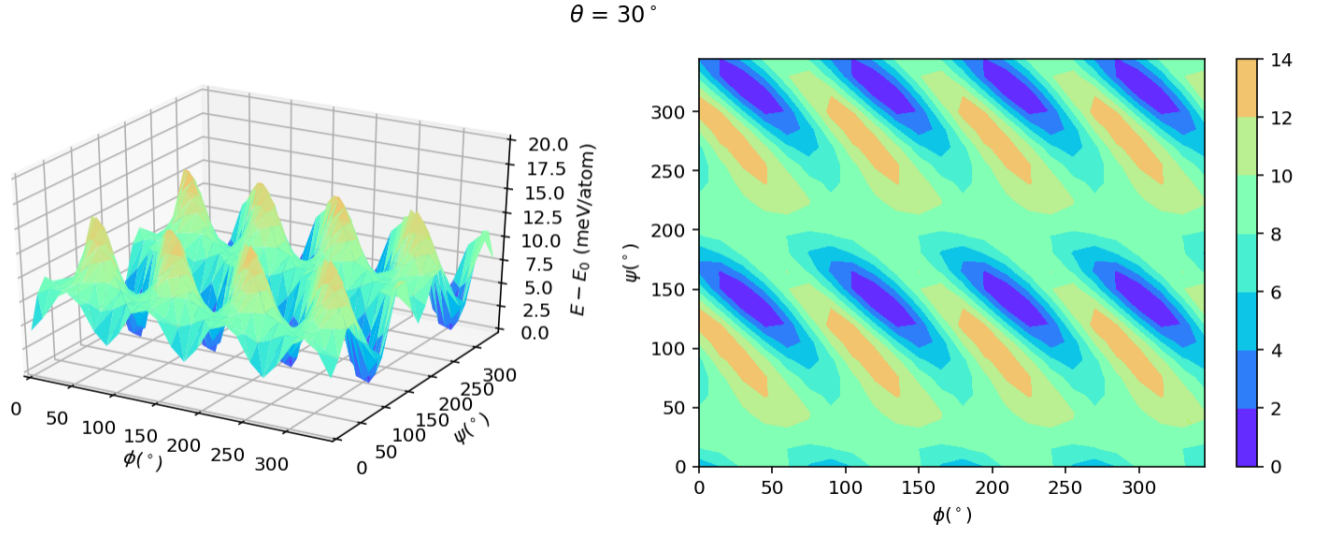


FIG. S7: Energy landscape corresponding to $E(\phi, \theta = 30^\circ, \psi)$

distribution. Not only are relationships between parameters related to each other through this representation, each data range is also demonstrated, e.g. $C - Bi$ bond-length is within the range $4.8 - 6.1 \text{ \AA}$.

* Electronic address: Annop.E@chula.ac.th

† Electronic address: Thiti.B@chula.ac.th

- [1] Y.-Y. Sun, J. Shi, J. Lian, W. Gao, M. L. Agiorgousis, P. Zhang, and S. Zhang, *Nanoscale* **8**, 6284 (2016).
- [2] E. J. Wegman, *Journal of the American Statistical Association* **85**, 664 (1990).

$\theta = 45^\circ$

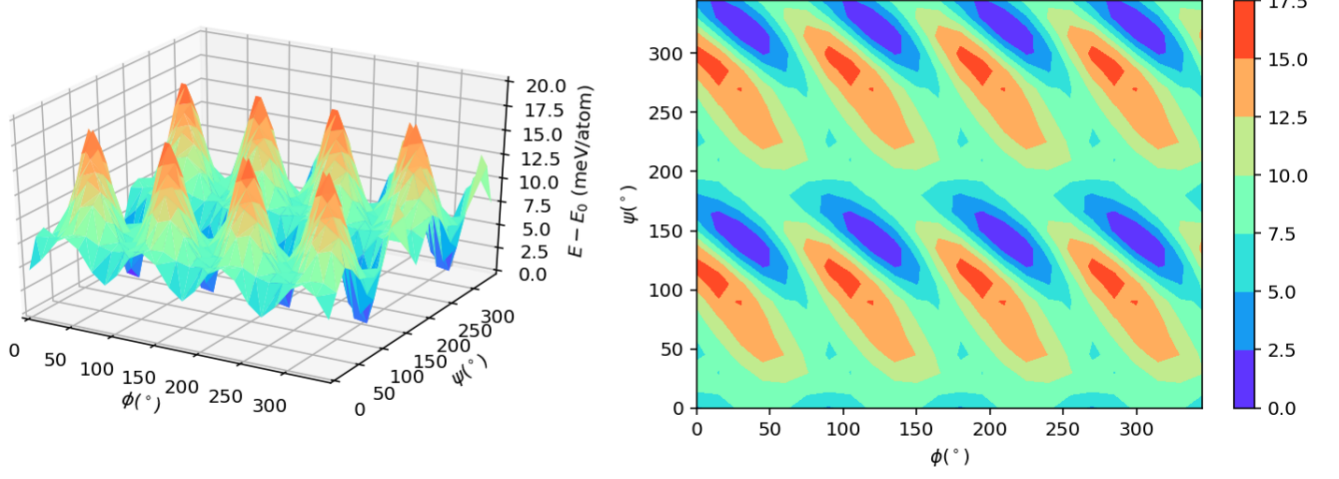


FIG. S8: Energy landscape corresponding to $E(\phi, \theta = 45^\circ, \psi)$

$\theta = 90^\circ$

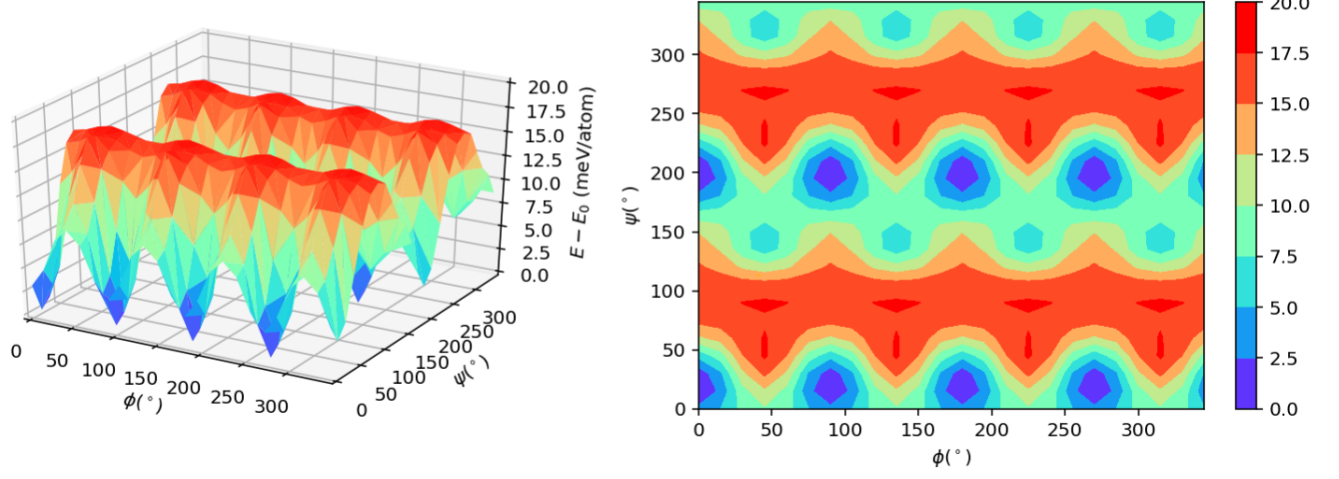


FIG. S9: Energy landscape corresponding to $E(\phi, \theta = 90^\circ, \psi)$

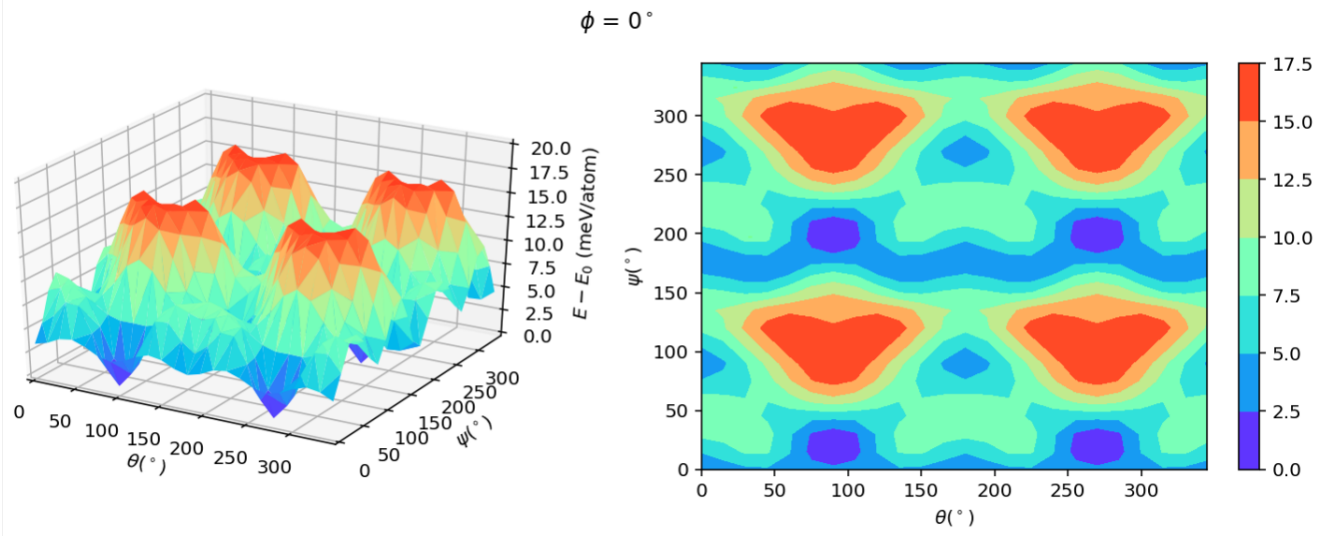


FIG. S10: Energy landscape corresponding to $E(\phi = 0^\circ, \theta, \psi)$

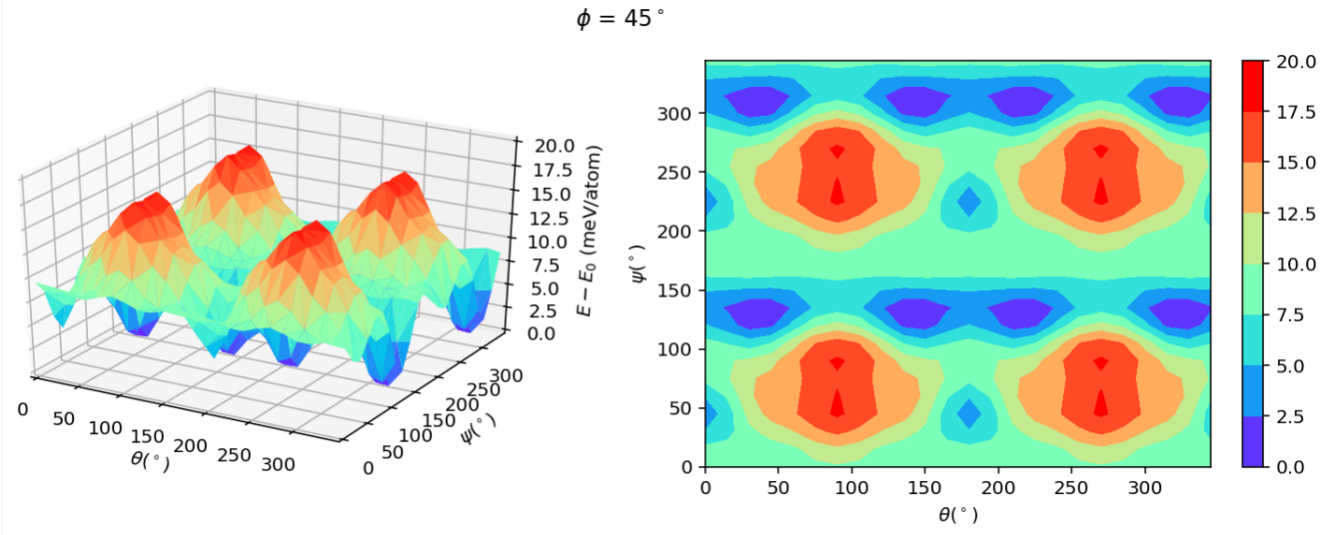


FIG. S11: Energy landscape corresponding to $E(\phi = 45^\circ, \theta, \psi)$

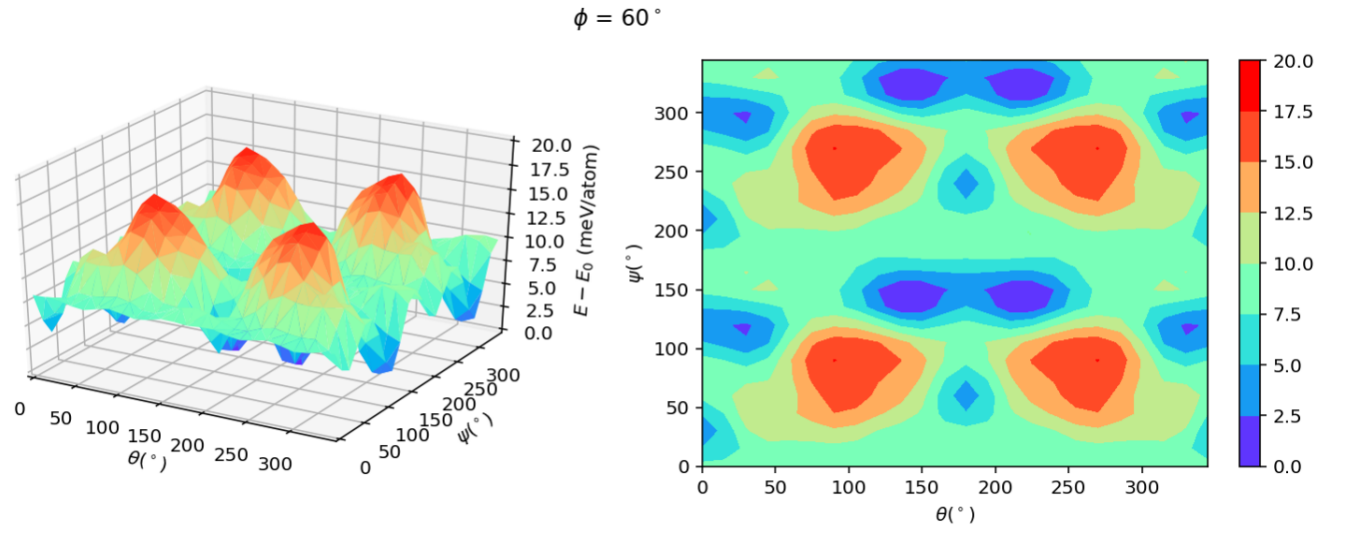
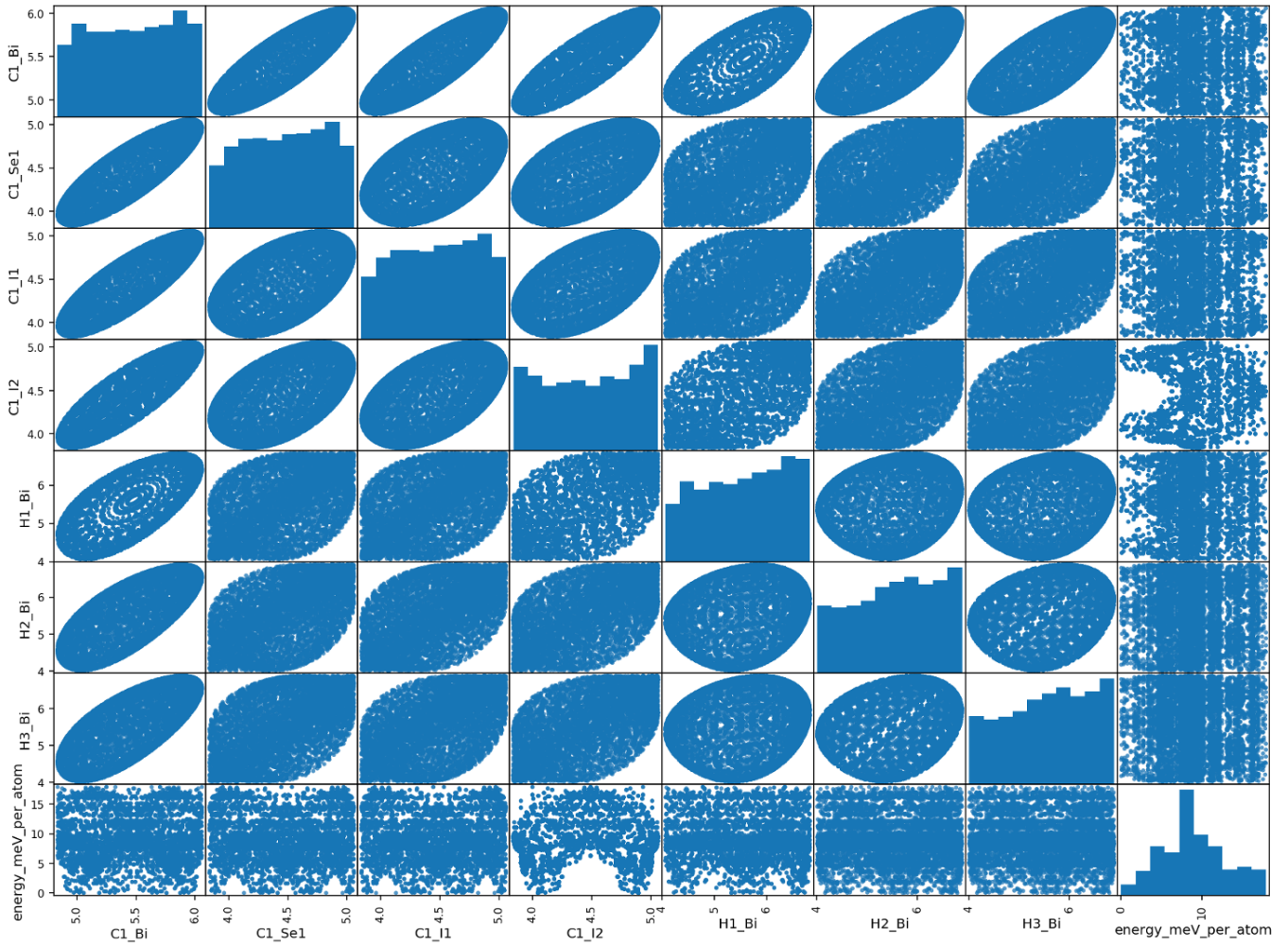


FIG. S12: Energy landscape corresponding to $E(\phi = 60^\circ, \theta, \psi)$



	C1_Bi	C1_Se1	C1_I1	C1_I2	H1_Bi	H2_Bi	H3_Bi	energy_meV_per_atom
C1_Bi	1.000000	0.790254	0.790254	0.865648	0.641726	0.696120	0.697059	-0.000019
C1_Se1	0.790254	1.000000	0.399610	0.546770	0.507357	0.544788	0.555839	-0.005765
C1_I1	0.790254	0.399610	1.000000	0.546770	0.507412	0.554999	0.545584	-0.005767
C1_I2	0.865648	0.546770	0.546770	1.000000	0.555245	0.603063	0.603733	0.010483
H1_Bi	0.641726	0.507357	0.507412	0.555245	1.000000	0.183782	0.184301	0.000113
H2_Bi	0.696120	0.544788	0.554999	0.603063	0.183782	1.000000	0.205890	0.000271
H3_Bi	0.697059	0.555839	0.545584	0.603733	0.184301	0.205890	1.000000	0.000147
energy_meV_per_atom	-0.000019	-0.005765	-0.005767	0.010483	0.000113	0.000271	0.000147	1.000000

FIG. S13: bondlengths (\AA) vs energy; bivariate correlations for all permutations

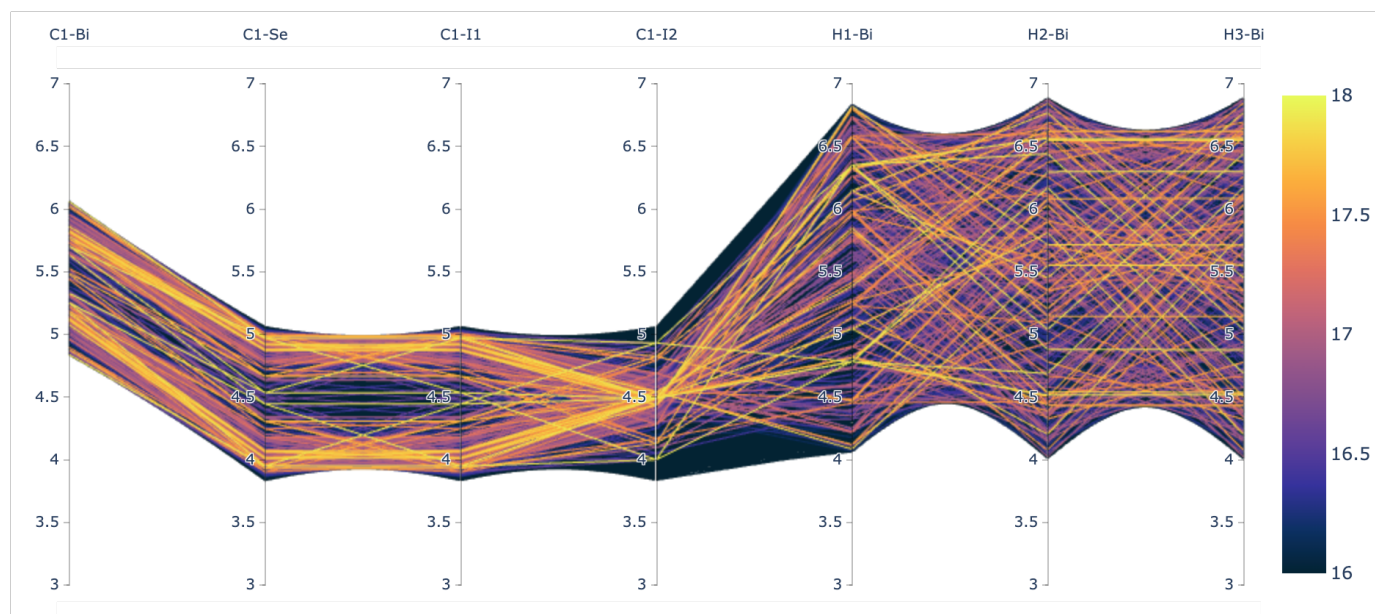


FIG. S14: Parallel coordinate representation of some selected pairs of bondlength